International Journal For Technological Research In Engineering
Volume 7, Issue 8, April-2020 *ISSN (Online): 2347 - 4718*

TEXTILE DYE REMOVAL USING PHOTOCATALYTIC CASCADE DISC REACTOR COATED BY CERIUM OXIDE NANOPARTICLES

Herbert Shyji A[1], Dr. J.Jeyanthi[2]
[2]Professor, [1,2]Department of Environmental Engineering, Government College of Technology, Coimbatore-641013, Tamilnadu, India,

Abstract: ***This paper reports the efficiency of the photocatalysis of CeO2 nanoparticles in degrading binary mixtures of Blue R4b and Red Rab dyes. A cascade disc reactor was designed for investigating the degradation of Blue R4b and Red Rab dye under UV radiation. Cerium oxide nanoparticles were synthesized by co-precipitation method and their properties were characterized by Particle size analyser, Fourier transform infrared spectroscopy (FTIR). Scanning electron microscopy (SEM), X-ray diffraction (XRD), BET surface area analyser and UV-Vis spectrophotometer. Different parameters like flowrate, dye concentration and pH were varied and their impact on dye degradation was studied. First order derivative spectrophotometric method was developed for the analysis of Blue R4b and Red Rab in mixed dye aqueous solution to overcome the limitations arising due to interference in the zero order spectral method.***

Keywords: Photocatalysis, CeO2 nanoparticles, Dye degradation,

I. INTRODUCTION

Today more than 10000 dyes are available in the market and are used in a wide range of applications like food, paper, rubber, plastics, cosmetics, leather and textiles industries. A large quantity of highly coloured wastewater containing artificial dyes and admixtures were generated from these industries and are discharged directly into nearby streams and rivers without proper treatment.[4-6]This results in an adverse impact on the Ecosystem, hence dye degradation is the main concern among researchers. The different process was used for the treatment of dye effluent, among them, Photocatalytic degradation is a prominent method which completely mineralize the pollutants.[2,3]When the suitable light source is used the photons collide with the surface of a photocatalyst, the electrons shifts from the valence band and transferred to the conduction band. As a result, the positive holes (h+) are generated in the valence band and react with the hydroxylated surface to produce OH• radicals. OH• radical is the most powerful oxidizing agent which degrade the pollutants effectively.

$$MO + h\nu \rightarrow MO\ (h^+ + e^-)$$

Oxidative reactions due to photocatalytic effect:

$$h^+ + H_2O \rightarrow H^+ + \bullet OH$$

$$2h^+ + 2\ H_2O \rightarrow 2\ H^+ + H_2O_2\ H_2O_2 \rightarrow 2\ \bullet OH$$

Reductive reactions due to photocatalytic effect:

$$e^- + O_2 \rightarrow \bullet O_2^-$$

$$\bullet O_2^- + H_2O + H^+ \rightarrow H_2O_2 + O_2$$

$$H_2O_2 \rightarrow 2\ \bullet OH$$

In this work, cerium oxide is used as photocatalyst which is the most abundant rare earth metal which has less energy difference among lower (Ce3+) and higher (Ce4+) ions. Cerium oxide has superior oxygen mobility and storage capacity and also has attractive optical possessions and photogenerated charge carriers.[5-6] These property makes Cerium oxide a superior material among the researchers which are used in various fields like optoelectronics, Catalyst in Fuel cells, gas sensors, Solid state electrolytes. In this study, Photocatalytic Cascade Disk Reactor coated with CeO_2 nanoparticle was used to study the removal efficiency textile dyes. Blue R4b and Red Rab dyes (commercial dyes) were used as a model dye to test a novel photocatalytic reactor. The reactor, contain plexiglass plates coated with CeO_2 nanoparticles. Dye degradation was monitored by measuring UV absorbance.

II. EXPERIMENTAL DETAILS

A. Materials and methods

Analytical grade of cerium nitrate, sodium hydroxide, hydrochloric acid obtained from Merck and mixed solvent (ethanol and water V/V ratio of 30:70). All experiments were carried out with Milli Q ultrapure water system of 18.2Ω resistivity.

B. Synthesis of cerium oxide nanoparticles

CeO_2 nanoparticle was synthesized using co-precipitation method. 1N sodium hydroxide is added dropwise to the precursor 0.1 M cerium nitrate which was prepared using mixed solvent (ethanol and water V/V ratio of 30:70). The solution was stirred at 250rpm at 60◦C, a white precipitate was formed. After the complete addition of NaOH, the solution was turned to pink colour. It indicates the complete oxidation of Ce(III) to Ce(IV). The final solution was stirred for 12 hours and a yellow precipitate was formed. Then the solution was centrifuged 10 minutes at 5000rpm and washed with ethanol and deionized water several times to remove excess ions. The obtained products were dried in a hot air oven at 70°c overnight and then calcined for 4 hours at 550°c. The cerium oxide nanoparticle was obtained which was used for further studies.[7][13][14]

C. Characterization

The structural morphology and composition of CeO_2 were investigated by Field Emission Scanning Electron Microscope (FESEM) coupled with EDAX. The BET specific surface area, pore volume and pore diameter of the sample was measured using Belsorp mini II surface area analyzer. The samples were degassed at 200°C to remove

moisture and impurity for 4 hours and their BET area, pore volume and pore diameter were determined. The Fourier Transform Infrared spectra of the CeO_2 nanoparticle was obtained using Perkin Elmer FTIR in the range of 4000-450 cm-1.

The UV-vis absorbance spectra of the samples were obtained by Perkin Elmer Lambda35 with a glass slit width of 1 nm. The samples were recorded at room temperature in the air within the range of 200-700 nm. X-ray powder diffraction(XRD) was used to measure the crystallite size and crystallite phase of the CeO_2 which was carried using Rigaku miniflex 6^{th} generation benchtop X-ray diffractometer.

D. Cascade Disc Reactor Setup

To degrade the dye, a photocatalytic cascade disc reactor is constructed, which consists of three 20 cm diameter circular disc made of Plexiglas and immobilized with CeO_2 nanoparticles. The dye solution was pumped from the top disc, and then it is transferred as cascade flow to lower level discs by small holes provided on each disc (12 small holes with 4 mm diameter). Also, the dyes are spontaneously aerated and pumped using a peristaltic pump which controls the flow rate. A UVC 20 W lamp is placed at the centre of the reactor, and disc beds are spray coated by CeO_2 nanoparticles.[1]

III. RESULTS AND DISCUSSION

A. Particle Size distribution and Zeta potential analysis:

The particle size of CeO_2 nanoparticle was determined using photon correlation spectroscopy. This method considers the shape of all particles as spherical and are called the hydrodynamic diameter. The particle size distribution greatly depends on Zeta potential value. greater the zeta value the particles are more stable. The Zeta values for the synthesized CeO_2 nanoparticle is -18.9 mV which shown in fig. 3. The particle size distribution was given in fig 2. The average particle size was found to be 242.1 nm. This show the particles undergoes agglomeration which increases the particle size.

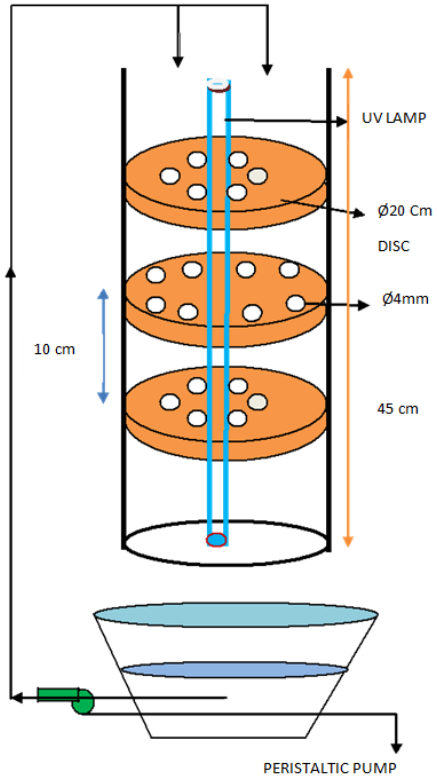

Fig. 1 Experimental setup

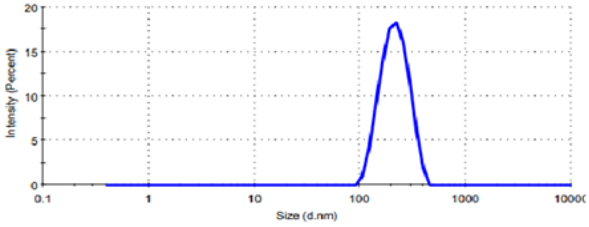

Fig. 2 Particle size distribution of CeO_2

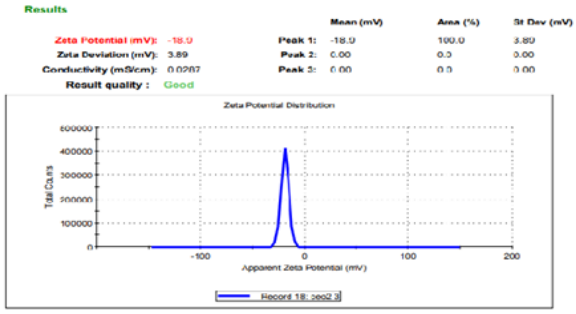

Fig. 3 Zeta potential of CeO_2

B. FTIR Analysis:

Fig. 4 shows the FT-IR spectra of CeO_2 nanoparticle. The peak at 3562.57 cm^{-1} corresponds to –OH stretching due to alcohols and the peak at 2820 cm^{-1} corresponds to N-H Stretching amine. The peak at 2349 cm^{-1} corresponds to O=C=O Stretching of CO_2 and the peak at 1519 cm^{-1} corresponds to N-O Stretching nitro compounds. The peak at 1381 cm^{-1} corresponds to C-H Bending Aldehydes and Alkalis. The Ce-O stretching band around 401 cm^{-1} confirms the fingerprint region of cerium oxide nanoparticle.[11,12]

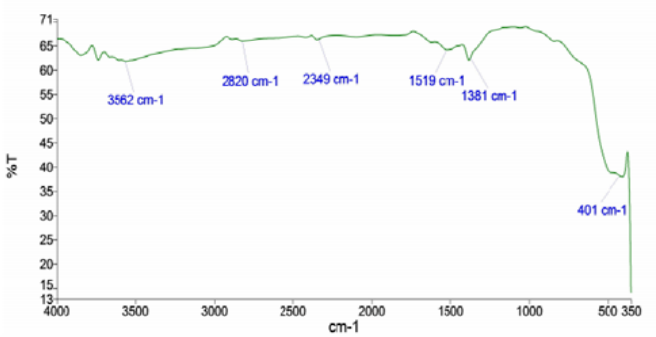

Fig. 4 FTIR analysis of CeO_2

C. UV Analysis :

The optical property of the CeO_2 was measured using UV spectroscopy in the range of 200 to 700 nm is shown in figure 5. The maximum peak obtained from the UV –VIS graph (λ_{max}) is at 302.4 nm. The Tauc plot was used to calculate the band gap

E=h *c/λ

Where, Energy (E) is Band gap, Velocity of light (c) is 2.99 * 10^8 meter/sec, wavelength(λ) is 302.4 nm, Plank's constant(h) is 6.626 * 10^{-34} Joules sec, 1 eV 1.6 * 10^{-19} Joules (conversion factor). Energy band gap width is calculated for the obtained 302.4 nm as 4.11 eV[13]

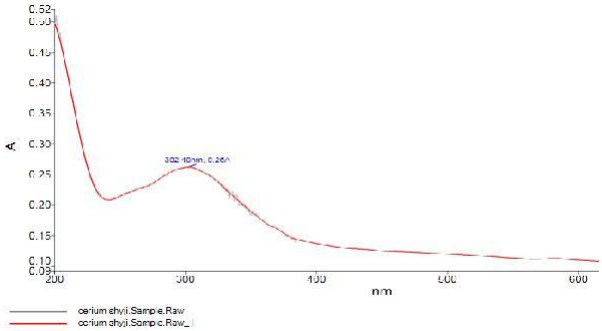

Fig 5 UV-Vis analysis of ceo_2

D. SEM analysis:

Scanning Electron Microscopy (SEM) provides insights about the morphology and size details of the nanoparticles. The surface morphology of the prepared CeO_2 is shown in figure 6. The image clearly shows the particles are spherical and are agglomerated in nature.

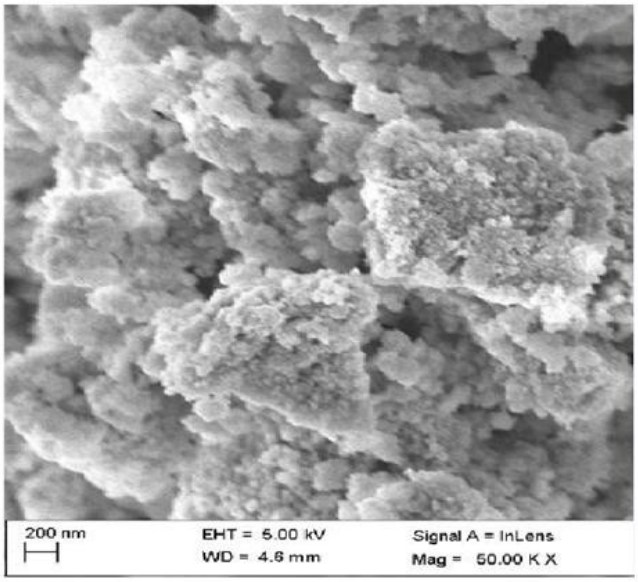

Fig. 6 SEM image of CeO_2

E. XRD analysis:

The structure of CeO_2 and their crystallite size were confirmed using powder XRD measurements. The XRD pattern of the CeO_2 nanoparticle is shown in figure 7. The results show diffraction peaks corresponds to hkl planes (111), (200), (220), (311), (222), (331), and (420). This pattern matches JCPDS-34-0394 which corresponds to the fine crystalline and cubic structure of CeO_2. The crystalline size (D) was calculated using the Scherrer formula,

$$= \text{Cos}$$

where D is the diameter of the particle, k is a constant (0.89), is the X-ray wavelength(0.154 nm), is the half diffraction angle and is the full width at half maximum. The crystallite size for peak maxima is found to be 6.4 nm.[11,12,14]

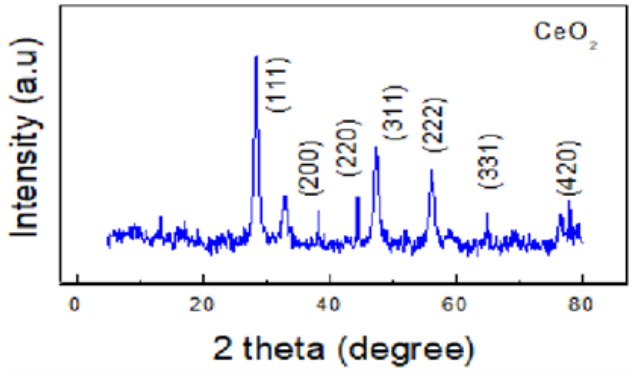

Fig. 7 XRD analysis of CeO_2

F. BET Surface Area Analysis

Fig. 8 shows the nitrogen adsorption-desorption is other ms at temperature 77 K. The isotherm of the sample reveals type IV adsorption isotherm which is mesoporous in nature. The BET surface area and pore nature of the sample were found using BET analysis. The surface area of the sample was calculated as 21.89 m^2/gm. Also, the pore volume and pore diameter were measured to be 0.1049 cm^3/gm and 14.517 nm respectively.

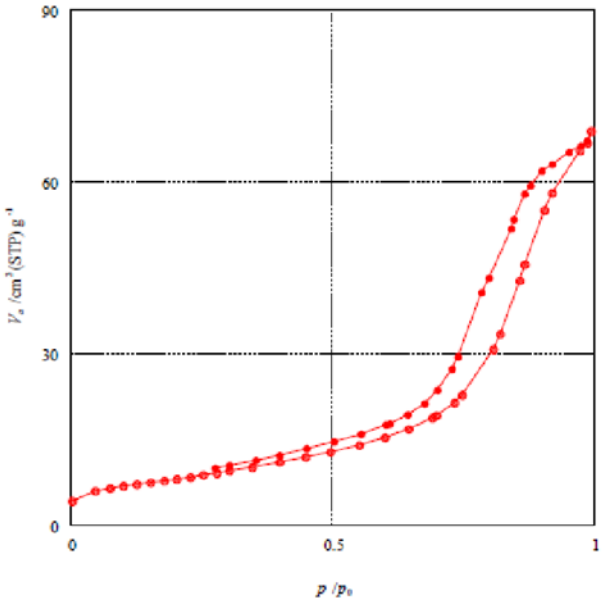

Fig 8. Adsorption and Desorption isotherm

G. Analysis of concentrations in mixed dye aqueous solutions:

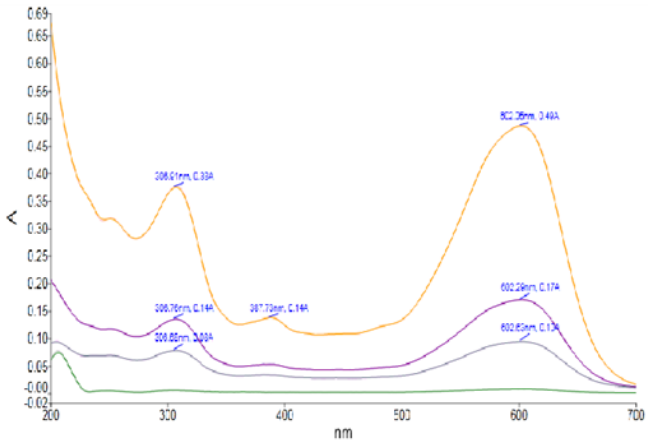

Fig .9 wavelength(λ_{max}) of Blue R_{4b}

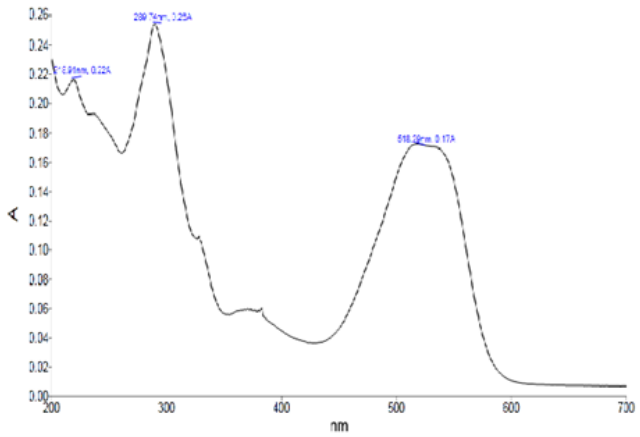

Fig. 10 wavelength (λ_{max}) of Red R_{ab}

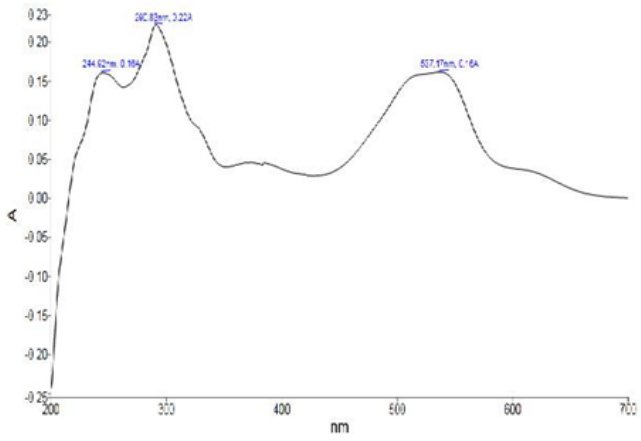

Fig. 11 wavelength(λ_{max}) of mixed dye

The single dye aqueous solutions of Blue R_{4b} and Red R_{ab} with known initial concentrations of 50 and 130 mg/L were prepared, and the zero-order absorption spectra of these single dye aqueous solutions were recorded between 602 and 518 nm and are presented in Fig 9 and Fig 10. As it can be observed from Fig.9 and Fig.10, the wavelength for maximum absorption (λmax) of Blue R_{4b} and Red R_{ab} was determined as 602 and 518 nm, respectively. For the simultaneous analysis of Blue R_{4b} and Red R_{ab} dyes in an aqueous solution of the two dyes, the mixed dye aqueous solution containing 50 mg/L of blue R_{4b} and 130 mg/L of Red R_{ab} were prepared and zero-order absorption spectra were recorded between 518 to 602nm (Fig. 11). As it can be observed from Fig. 11, the spectra for Blue R_{4b} and Red R_{ab} show two peaks at 518 and 602 nm. However, in comparison of Fig. 9 and 10 with Fig. 11, it is observed that the absorbance values with dual dye spectra at 518 and 602 nm are different than those in the corresponding single dye spectra. This is due to overlap of the absorbance by both the dyes, indicating the interference between the zero-order spectra of Blue R_{4b} and Red R_{ab} dyes. Hence, by direct absorbance measurement concentrations of the model dyes could not be determined. Derivative spectrophotometry can be with overlapping spectra. The derivation of the zero-order spectrum can lead to separation of overlapped signals, which reduces the effect of spectral background interferences caused by the presence of other compounds in a sample. Thus, the simultaneous analysis of Blue R_{4b} and Red R_{ab} dyes were carried out using the first-order derivative spectrophotometric method. The derivative spectrophotometric method was used in the present work for the simultaneous analysis of Blue R_{4b} and Red R_{ab} dye in mixed dye solutions, using zero-crossing point of first-order derivative spectra. The variations of first-order derivative absorption spectra of Blue R_{4b} and Red R_{ab} in single and mixed dye solutions with wavelength are presented in Fig. 12. As it can be observed from Fig.12, the first-order derivative spectra of Blue R_{4b} and Red R_{ab} dyes in the single dye solution and mixed dye solutions showed that Blue R_{4b} absorbance can be determined at 640 nm in the presence of Red R_{ab}, where the derivative of absorbance of Red R_{ab} is zero and Red R_{ab} dye can be determined at 375 nm in the presence of Blue R_{4b} , where the derivative of absorbance of Blue R_{4b} dye is zero (Fig. 12).

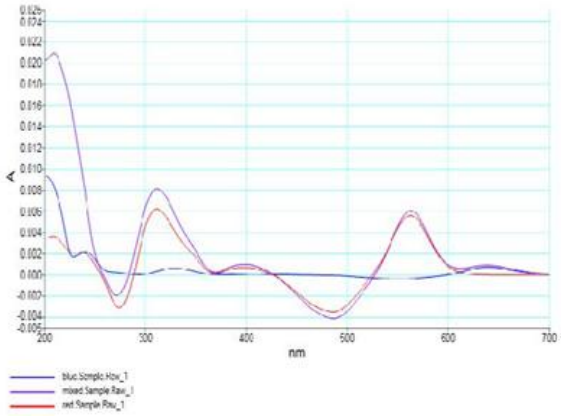

Fig. 12 First-order derivative absorption spectra of Blue R_{4b} and Red R_{ab} in single and mixed dye solutions with the wavelength

The calibration equations for Blue R_{4b} and Red R_{ab} dyes at these individual wavelengths (640and 375 nm) were

separately obtained to determine the concentration of each dye in the mixture. Thus, to determine the dye concentrations in mixed dye aqueous solutions, UV–Vis spectrophotometer was calibrated at 640 nm for Blue R_{4b} and 375 nm for Red R_{ab}. The concentrations of Blue R_{4b} and Red R_{ab} in unknown samples with a mixture of these dyes in aqueous solutions were measured by measurement of absorbance after suitable dilution using UV–Vis spectrophotometer at 640 for Blue R_{4b} analysis and 375 nm for Red R_{ab} analysis followed by determination of concentration using the corresponding calibration followed by multiplication with dilution factors.

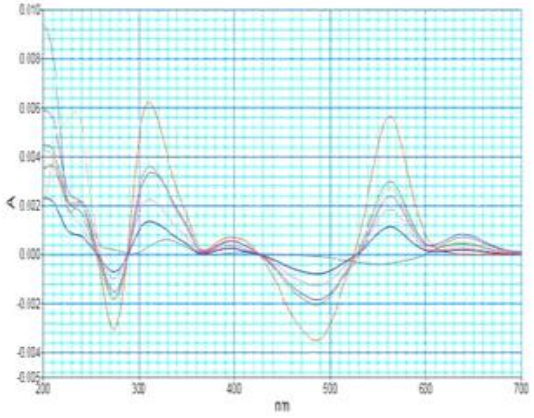

Fig. 13 Derivatives of absorbance of Blue R_{4b}

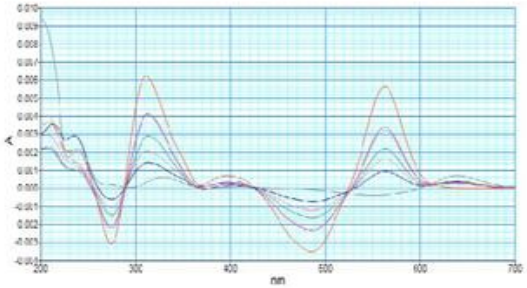

Fig. 14 Derivatives of absorbance of Red R_{ab}

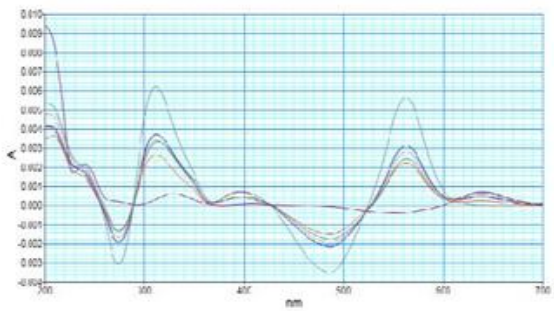

Fig.15 Derivatives of absorbance of Blue R_{4b} and Red R_{ab}

H. Effect of pH

The pH is an important variable in evaluating the performance of Photocatalytic degradation. The study of the influence of pH was studied for the pH 5,7, and 9 under the conditions 20 ppm initial concentration, flow rate 8 cc/sec. At lower pH, the dyes start to decolourize naturally and hence the lower pH was avoided. The effect of pH on the photocatalysis of Model dyes are shown in fig 16. It is known the Pzc of CeO_2 corresponds to 0.001 M KCL solution is 5.2. Below this point, the surface of the nanocomposite will be positively charged which enhances the negatively charged model dyes through electrostatic force of attraction. This reduces the ability of the photocatalysis which is shown in figure 16 At pH 5 the attractive forces are lesser and the higher dye degradation efficiency is achieved. Whereas in pH 9 the there exist a strong repulsive force among the dye and catalyst the efficiency of dye degradation is decreased. [13,15]

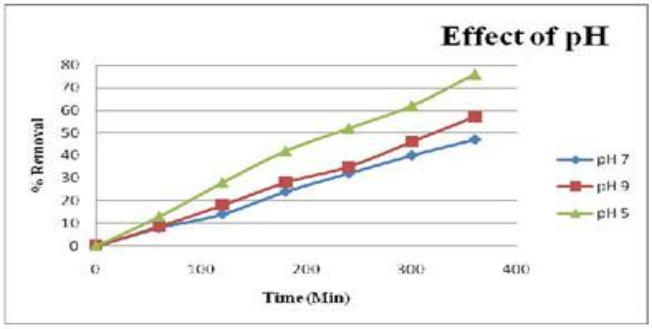

Fig. 16 Effect of pH

(Initial dye concentration 20 ppm, Flow rate 8 cc/sec)

I. Effect of Initial dye Concentration

Initial dye concentration is an important parameter in the photocatalytic process. Fig. 17 shows the effect of various initial dye concentrations 10, 25 and 50 ppm on the photocatalytic process. The results shown in figure 17 illustrates that an increase in the dye concentration will lower the removal rate. When the initial dye concentration increases from 10 to 20 and 50 ppm, the degradation efficiency of model dyes decreased from 80.3 % to 47 %. This may have resulted in the shortage of reactive species with increasing dye concentration, there exists a competition with the reactive species which decreases the degradation efficiency.[13,17]

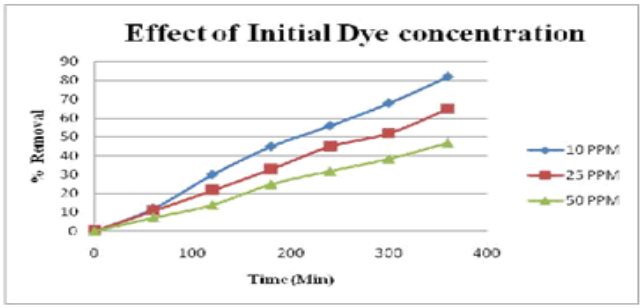

Fig. 17 Effect of Initial dye concentration

(Flow rate 8 cc/sec, pH 5)

J. Effect of Flow rate

The effects of flow rate on the model dye removal were also evaluated. These experiments use dye concentrations of 10 ppm; and flow rates of 4, 6 and 8 cc/sec. The results are shown in the fig. 18 which shows at a higher flow rate, the rate of degradation is high. This is due to the fact at a higher

flow rate the more dye particle will collide with the catalyst at high velocity which results in higher degradation. Also at higher flow rate the diffusion phenomenon happens between the catalyst and dye particle and increases the mass transfer. This results in higher degradation of the model dye[1].

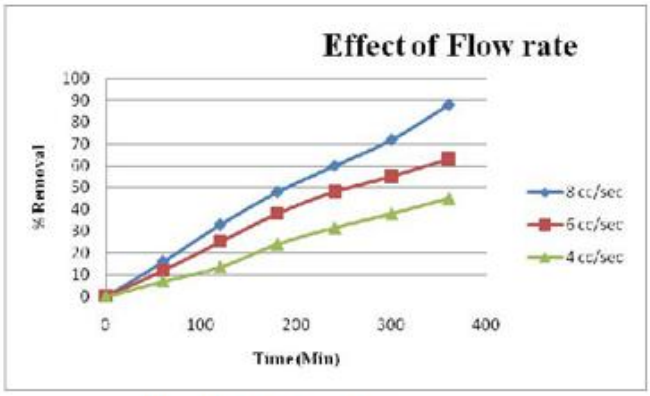

Fig. 18 Effect of Flow rate

(Initial concentration 10 ppm, pH-5)

IV. CONCLUSION

The cerium oxide photocatalyst was prepared through the Co-precipitation method. The formation of CeO_2 nanoparticles was confirmed by X-ray diffraction (XRD). The FT-IR spectrum indicated the presence of different functional groups and confirms the presence of Cerium in its finger print region. The morphology and the size of the cerium oxide nanoparticles were characterized using Scanning Electron Microscopy and the optical properties were studied by the UV-Visible absorption spectrum. A cascade disc reactor was designed to degrade the selected blue R_{4b} and red R_{ab} dyes. The operational parameters were optimized and the following condition was suggested to obtain maximum degradation: pH: 5, solution concentration: 10 ppm, and flow rate 8 cc/sec. In this work we achieved 88% degradation under optimum conditions after 360 minutes of irradiation. Based on the previously mentioned experiments and characterization it could be concluded that Cerium oxide catalyst prepared could be efficiently used for the degradation of dyes using a cascade disc reactor.

REFERENCES

[1] H. Amiri, B. Ayati, and H. Ganjidoust, "Textile Dye Removal Using Photocatalytic Cascade Disk Reactor Coated by ZnO Nanoparticles", J. Mater. Sci. Chem. Eng., vol. 04, no. 12, pp. 29–38, 2016.
[2] W. Guo, Z. Yang, X. Zhou, and Q. Wu, "Degradation and mineralization of dyes with advanced oxidation processes (AOPs): A brief review", in Proceedings of the 2015 International Forum on Energy, Environment Science and Materials, Shenzen, China, 2015.
[3] S. S. Kalra, S. Mohan, A. Sinha, and G. Singh, "Advanced Oxidation Processes for Treatment of Textile and Dye Wastewater", p. 5.
[4] S. S. Lakshmi, "Removal of organic pollutants from textile dye wastewater by advanced oxidation process", p. 10.
[5] S. W. Lewis, "Chapter 11: Analysis of dyes using chromatography",‖ p. 20.
[6] D. Novitasari, R. Sauriasari, and M. Kurniadi, Analysis of synthetic red dyes in red spinach samples (amaranthus tricolour l.),‖ Int. J. Appl. Pharm., vol. 10, no. 1, p. 15, Dec. 2018.
[7] C. Benmouhoub, A. Kadri, N. Benbrahim, and S. Hadji, "Synthesis and Characterization of Cerium Oxide (CeO2) Nanoparticles",‖ Mater. Sci. Forum, vol. 609, pp. 189–194, Jan. 2009.
[8] S. Durmus, A. Dalmaz, M. Ozdincer, and S. Sivrikaya, "Preparation of Cerium Oxide Nanoparticles: An Efficient Catalyst to the Synthesis of Dimeric Disulphide Schiff Bases",‖ vol. 13, no. 1, p. 6, 2017.
[9] M. Farahmandjou and M. Zarinkamar, "Synthesis of nano-sized ceria (CeO2) particles via a cerium hydroxy carbonate precursor and the effect of reaction temperature on particle morphology",‖ p. 6, 2015.
[10] M. Farahmandjou, M. Zarinkamar, and T. P. Firoozabadi, "Synthesis of Cerium Oxide (CeO2) nanoparticles using simple CO-precipitation method",‖ Rev Mex Fis, p. 5, 2016.
[11] K. Kaneko et al., "Structural and Morphological Characterization of Cerium Oxide Nanocrystals Prepared by Hydrothermal Synthesis",‖ Nano Lett., vol. 7, no. 2, pp. 421–425, Feb. 2007.
[12] P. Kavitha, R. Ramesh, M. R. Rajan, and C. Stella, "Synthesis and Characterization of Cerium Oxide Nanoparticles by Using Rapid Precipitation Method"‖ p. 3, 2015.
[13] K. Sridevi Lakshmi, J. Jeyanthi and R. Bhuvaneswari," Photocatalytic Degradation of Allopurinol using Cerium Oxide", The Asian Review of Civil Engineering, p. 39-44
[14] M. Ramachandran, M. Shanthi, R. Subadevi, and M. Sivakumar, "Role of surfactant on synthesis and characterization of cerium oxide (CeO2) nanoparticles by modified co-precipitation method",‖ vol. 04, no. 09, p. 5, 2017.
[15] P. Reshma and K. Ashwini, ―Cerium Oxide Nanoparticles: "Synthesis, Characterization and Study of Antimicrobial Activity", J. Nanomater. Mol. Nanotechnol., vol. 06, no. 03, 2017. 43
[16] Younis, D. Chu, and S. Li, "Cerium Oxide Nanostructures and their Applications", Functionalized Nanomaterials,
[17] Use of cerium oxide (CeO2) nanoparticles for the adsorption of dissolved cadmium (II), lead (II) and chromium (VI) at two different pHs in single and multi-component systems,‖ Glob. NEST J., vol. 17, no. 3, pp. 536–543, Aug. 2015.

